1330–1344 *Nucleic Acids Research, 2017, Vol. 45, No. 3* *Published online 15 December 2016*
doi: 10.1093/nar/gkw1264

A specific dsRNA-binding protein complex selectively sequesters endogenous inverted-repeat siRNA precursors and inhibits their processing

Thomas Montavon[1], Yerim Kwon[1], Aude Zimmermann[1], Philippe Hammann[2], Timothée Vincent[1], Valérie Cognat[1], Fabrice Michel[1] and Patrice Dunoyer[1,*]

[1]Université de Strasbourg, CNRS, IBMP UPR 2357, F-67000 Strasbourg, France and [2]Université de Strasbourg, CNRS, IBMC FRC1589, Plateforme Protéomique Strasbourg - Esplanade, F-67000 Strasbourg, France

Received July 25, 2016; Revised December 01, 2016; Editorial Decision December 02, 2016; Accepted December 06, 2016

ABSTRACT

In plants, several dsRNA-binding proteins (DRBs) have been shown to play important roles in various RNA silencing pathways, mostly by promoting the efficiency and/or accuracy of Dicer-like proteins (DCL)-mediated small RNA production. Among the DRBs encoded by the *Arabidopsis* genome, we recently identified DRB7.2 whose function in RNA silencing was unknown. Here, we show that DRB7.2 is specifically involved in siRNA production from endogenous inverted-repeat (endoIR) loci. This function requires its interacting partner DRB4, the main cofactor of DCL4 and is achieved through specific sequestration of endoIR dsRNA precursors, thereby repressing their access and processing by the siRNA-generating DCLs. The present study also provides multiple lines of evidence showing that DRB4 is partitioned into, at least, two distinct cellular pools fulfilling different functions, through mutually exclusive binding with either DCL4 or DRB7.2. Collectively, these findings revealed that plants have evolved a specific DRB complex that modulates selectively the production of endoIR-siRNAs. The existence of such a complex and its implication regarding the still elusive biological function of plant endoIR-siRNA will be discussed.

INTRODUCTION

In eukaryotes, RNA silencing is a conserved mechanism that plays essential roles in many biological processes such as maintenance of genome stability, development or antiviral defense. The various classes of endogenous or exogenous 21–24 nucleotide (nt) small RNA (sRNA), which confer the sequence specificity of this mechanism, are produced from structurally distinct double-stranded RNA (dsRNA) precursors by RNaseIII-like enzymes called Dicers, or Dicer-like (DCL) in plants (1–3). The plant model *Arabidopsis thaliana* encodes four DCL proteins with specialized functions. DCL1 produces the majority of micro RNAs (miRNAs) from relatively short imperfect stem-loop RNA precursors, whereas populations of 21, 22 and 24 nt short-interfering RNAs (siRNAs) are generated through the action of DCL4, DCL2 and DCL3, respectively, on various dsRNA substrates. For instance, DCL4-dependent 21 nt trans-acting (ta-)siRNAs are produced by sequential processing of long dsRNA precursors generated by the action of RNA-dependent RNA polymerase 6 (RDR6) on single-stranded RNA (4–6). By contrast, DCL3-dependent 24 nt siRNAs, the most abundant class of sRNAs, are produced from short dsRNA precursors, 27–50 nt in length, generated by PolIV and RDR2 and are usually referred to as p4-siRNAs (7,8). Finally, long and RDR-independent dsRNA precursors, originating from several endogenous loci configured as inverted-repeat (IR) transcripts are processed by the three siRNA-producing DCLs to generate 21, 22 and 24 nt endogenous inverted-repeat-derived (endoIR-)siRNAs (3,9–11).

Upon processing, sRNAs are incorporated into an RNA-induced silencing complex containing 1 of the 10 Argonaute (AGO) proteins that effect RNA silencing in *Arabidopsis*. Most 21 and 22 nt sRNAs load into AGO1 to promote cleavage or translational inhibition of target transcripts (12–14), whereas 24 nt siRNAs associate with AGO4, AGO6 or AGO9 to guide heterochromatin formation by DNA methylation and histone modification (15). Infection by viruses also leads to production of, mostly, 21 and 22 nt virus-derived (v)siRNAs through processing by DCL4, or its surrogate DCL2, of dsRNA replication intermediates or intramolecular fold-back structures within viral genomes (16–18). These vsiRNA are mainly loaded into AGO1 and AGO2, which then target single-stranded viral RNA for cleavage (19–24).

In addition to Dicer or DCL proteins, several dsRNA-binding proteins (DRBs) have been shown to play impor-

*To whom correspondence should be addressed. Tel: +33 3 67155368; Fax: +33 3 67155300; Email: patrice.dunoyer@ibmp-cnrs.unistra.fr

tant roles in plant and animal RNA silencing pathways (25–28). The *Arabidopsis* genome encodes five DRBs (DRB1-5) that are strictly composed of two dsRNA-binding motif (dsRBM) with no other catalytic domain. Among those five, DRB1, also known as HYL1, is the best studied and was shown to be required for precise and efficient processing of miRNA precursors (27,29–31) and for selection of the miRNA guide strand loaded into RNA-induced silencing complex. These functions are achieved through DRB1 interaction with DCL1 *via* its second dsRBM (32–35), while the first dsRBM binds miRNA precursors as well as mature miRNA duplexes (30,36,37). DRB2 is also involved in processing miRNAs but only in the shoot apical meristem where it represses DRB1 transcription (38,39). Interestingly, DRB1 seems to be specifically required for miRNA-guided cleavage whereas DRB2 is required for miRNA-mediated translational inhibition, suggesting that the miRNA mode of action is, at least partly, defined by those two DRBs (39,40). The roles of DRB3 and DRB5 are more elusive. They have been shown to be dispensable for sRNA production but seem to be required for translational repression of DRB2-associated miRNA target transcripts (40,41). DRB3 was also found to interact with DCL3 and AGO4 and impact the methylation of a viral genome without being required for the processing of viral dsRNA by DCL3 (42). Finally, DRB4 is essential for DCL4 activity *in vitro* (43) and was shown to physically and functionally interact with DCL4 *in vivo* (35,44), where it is required for accurate and efficient processing of ta-siRNA precursors (44,45) and of the few DCL4-dependent miRNAs (46,47). DRB4 plays also a role in antiviral defense either by promoting DCL4-dependent vsiRNA production (41,48) or by regulating resistance (*R*) gene-mediated immunity (49). More intriguingly, DRB4 was also shown to affect the processing by DCL3 of p4-siRNA and IR-siRNA precursors, where the former is decreased whereas the latter is strongly increased in *drb4* mutant (47,50). However, this effect is most likely indirect given that DRB4 does not interact *in vivo* with DCL3 (47).

Besides those five DRBs containing two dsRBMs, we have recently identified a new DRB family (named DRB7) conserved in all vascular plants and harboring a single dsRBM that shows concerted evolution with the most C-terminal dsRBM of DCL4 (51). We showed that one of the two *Arabidopsis* DRB7 proteins (DRB7.2) interacts with DRB4 but does not seem to be required for the production of any DCL4-dependent sRNAs, including the newly identified class of epigenetically activated (ea)siRNAs that accumulate mostly in the vegetative nucleus of pollen grains or in Decreased DNA Methylation 1 (ddm1) mutants (52–56). By contrast, loss of DRB7.2 triggered an increase in the accumulation of DCL3-dependent 24 nt siRNAs from easiRNA-generating loci. However, given that this observation was only made in a *ddm1* mutant background, and considering the pleiotropic nature of this mutation, the reason of this change is still unclear, as is the function of DRB7.2 (51).

Using genetic, biochemical and small RNA profiling approaches, we show, here, that DRB7.2 negatively regulates the production of endogenous IR-derived siRNA through specific sequestration of their dsRNA precursors. This sequestration requires its interacting partner DRB4 and represses their processing by the siRNA-generating DCLs, chiefly DCL3. The present study also reveals that DRB4 is partitioned into two distinct cellular pools fulfilling different functions, through mutually exclusive binding with either DCL4 or DRB7.2 that accumulate in distinct subcellular compartments. Collectively, these results uncover the existence of a specific DRB complex that selectively modulates processing of endogenous IRs, unravelling further layers of complexity in the plant RNA silencing pathways.

MATERIALS AND METHODS

Plant materials, transformation and virus inoculation

Knock-out T-DNA mutant lines *dcl2-1* (SALK_064627), *dcl3-1* (SALK_005512), *dcl4-2* (GABI_160G05), *dcl2/dcl3*, *dcl2/dcl4*, *dcl3/dcl4*, *drb4-1* (SALK_000736) and missense mutant *dcl4-8* were described previously (44,50,57–60). The 35S-GFP line in Columbia ecotype (Col-0) was kindly provided by M. Jean Molinier (IBMP). The mutant *drb7.2* (GABI 525B11) was obtained from the Arabidopsis Biological Ressource Center (ABRC) and was described previously (51). *Arabidopsis thaliana* reference ecotype used was Columbia. Genotyping of the Transfer DNA (T-DNA) insertion lines was performed by polymerase chain reaction (PCR), using allele-specific primers. PCR primers are listed in Supplementary Table S1. The *drb7.2/dcl2*, *drb7.2/dcl3*, *drb7.2/dcl4*, *drb4/dcl2*, *drb4/dcl3* and *drb4/dcl4* mutant lines were generated by standard genetic crosses. Homozygous mutant genotypes were confirmed by allele-specific PCR assays after two generations.

Plant seeds were stratified for 2–4 days at 4°C before growth under standard conditions at 22°C with a 16 h light/8 h dark cycle, either in soil or on Murashige and Skoog (MS) agar plates suplemented with kanamycin (50 μg/ml), hygromycin (34 μg/ml) or with phosphinotricin (10 μg/ml). *Arabidopsis* were transformed using the floral dip method (61).

Binary vectors carrying the infectious clone of *Tobacco rattle virus*-PDS or *Turnip crinkle virus* were described previously (62,63). These vectors were mobilized into Agrobacterium strain GV3101 and used for virus infection in *Arabidopsis*. Infected systemic leaves were collected at 14 dpi.

DNA constructs

For the DRB7.2:GFP fusion protein, the genomic sequence of DRB7.2 (At4g00420), either alone or with a 3.5 kb region upstream of the ATG, containing its endogenous promoter, was amplified with DNA PHUSION polymerase (Thermo Scientific), cloned into pGEMT-easy vector (Promega) for sequencing and sub-cloned into pCTL1300 binary vector for transient expression to generate 35S-DRB7.2:GFP or pDRB7.2-DRB7.2:GFP constructs. For the DCL4:FHA/GFP contructs, the genomic coding sequence of DCL4 was cloned, in fusion with GFP or double-epitope tag (2xFlag 2xHA), as C-terminal fusions under the control of its endogenous promoter (1.5 kb upstream of the ATG), in pB7GW34 vector using the 'MultiSite Gateway Three- Fragment Vector Construction Kit' (Invitrogen).

RNA analysis

Total RNA was extracted from *Arabidopsis* tissues with Tri-Reagent (Sigma, St Louis, MO, USA) according to manufacturer's instructions. RNA gel blot analysis of high and low molecular weight RNA was on 5 and 45 μg of total RNA, respectively, and was conducted as described previously (64). Radiolabeled probes for detection of the IR71 and IR2039 siRNAs were made by random priming reactions (Promega) in the presence of α-^{32}P-dCTP. The template used was a 650-bp-long (for IR71) and 670-bp-long (for IR2039) PCR product amplified from the Arabidopsis gDNA. DNA oligonucleotides complementary to miRNAs, trans-acting siRNAs or heterochromatic siRNAs (Supplementary Table S1) were end-labeled with γ-^{32}P-ATP using T4 PNK (Thermo Scientific). Detection of the *Arabidopsis* U6 small nuclear RNA was used to confirm equal loading. Each result was, on average, confirmed on four independent biological replicates.

Protein extraction and analysis

Total proteins were extracted from *Arabidopsis* flower buds as previously described (65) and were resolved on SDS–PAGE. After electroblotting onto Immobilon-P membrane (Millipore), protein gel blot analysis was carried out using the appropriate antiserum. The specificity of DRB4, DCL4, DCL3, AGO1 and AGO4 antibodies used in this study has been verified by Western blot analysis on protein extracts from wild type and the corresponding T-DNA mutant plants (64). Each result was, on average, confirmed on three independent biological replicates.

Protein and RNA immunoprecipitation

For immunoprecipitation, 0.1 g of flower buds was ground in liquid nitrogen and homogenized in 1 ml of lysis buffer (50 mM Tris–HCl, pH 7.5, 150 mM NaCl, 1% Triton X-100) containing 1 tablet/50 ml of protease inhibitor cocktail (Roche) for 15 min at 4°C. Cell debris was removed by two successive centrifugations at 13 000 rpm at 4°C for 10 min. After the second centrifugation an aliquot of supernatants was taken for input fraction. The remaining extracts were incubated with magnetic microparticles coated with monoclonal GFP or HA antibodies (MACS purification system, Miltenyi Biotech) at 4°C for 30 min. Samples were passed through Mcolumn (MACS purification system, Miltenyi Biotech) and an aliquot of the flow-through fraction was taken. The Mcolumn were then washed 2 times with 500 μl of lysis buffer and 1 time with 100μl of washing buffer (20 mM Tris–HCl, pH 7.5). To elute the immunoprecipited proteins, 95°C pre-warmed Western blot loading buffer (10% glycerol, 4% SDS, 62.5 mM Tris-HCl pH 6.8, 5% (v/v) 2-β-mercaptoethanol, Bromophenol Blue) was passed through the Mcolumn. Proteins were analyzed by Western blotting. For RNA extraction from immunoprecipited proteins, magnetic beads were eluted with 50°C pre-warmed Tri-Reagent (Sigma, St Louis, MO, USA) and RNA were extracted according to manufacturer's instructions. RNA were analyzed by Northern blotting.

Real-time RT-qPCR

In all, 2 μg of total RNA samples were reverse-transcribed into cDNA using SuperScript III reverse transcriptase (Invitrogen) with a mix of oligo(dT) and random hexamers. The cDNA was quantified using a SYBR Green qPCR kit (Eurogentec) and DRB4 specific primers (Supplementary Table S1). PCR was performed in triplicate in 384-well optical reaction plates heated for 10 min at 95°C, followed by 45 cycles of denaturation for 15 s at 95°C, annealing for 20 s at 60°C and elongation for 40 s at 72°C. A melting curve was performed at the end of the amplification by steps of 1°C (from 53°C to 95°C). The number of cycles after which fluorescence reached a set threshold (Ct value) was averaged for each triplicate and expressed as a ratio to the actin-2 mRNA.

Sequencing and bioinformatic analyses

Total RNA from two independent biological replicate of Col-0 and *drb7.2* flowers was extracted with Tri-Reagent (Sigma). A 6 μg weight of total RNA was used for preparation of small-RNA libraries. Briefly, a first acrylamide gel purification of small RNA between 18–30 nt was performed. The libraries were then constructed using the TruSeq Small RNA preparation kit from illumina following manufacturer's instructions and the libraries were sequenced using a Illumina Genome Analyser (Fasteris, Switzerland). After removal of the 3′ adapters from the reads by Fasteris using an in-house developed script (detailed in the Supplementary Table S2), sequences (18–26 nt in length) were mapped using Bowtie (66) to the TAIR10 assembly. Only unique reads with no mismatch to the genome were kept using an in-house python script (avalailable upon request). Counts were made with intersetBed, from bedtools suite (v.2.25.0) (67). Data were normalized with there own conserved miRNA counts (miR156, 157, 159, 160, 162, 164, 165, 166, 167, 168, 169, 170, 171, 172, 319, 390, 391, 393, 394, 395, 396, 397, 398, 399, 403, 408, 472) (68) under the assumption that they were globally unaffected (Figure 2 and (51)). miRNA annotation was downloaded from miRBase v.21 (69). EndoIR-siRNAs were annotated using the sRNA-producing loci predicted by (10), which did not match miRBase miRNAs. Loci-producing siRNAs in a PolIV-dependent manner where retrieved from (70). Those data have been converted from TAIR6 to TAIR10 coordinates by a perl script provided by the 1001 genomes project (http://1001genomes.org/data/software/translate_tair8/) and manually validated. tasiRNA producing loci were given by tasiRNAdb (71). The data reported in this paper will be deposited in the Gene Expression Omnibus (GEO) database, www.ncbi.nlm.nih.gov/geo(accession no. GSE92309).

Imaging

Imaging of fluorescent protein fusions was performed in roots of 2 weeks old stably-transformed plants using confocal microscope LSM700 or LSM780 from Carl Zeiss with a 40x objective and a 488-nm laser for excitation. Images were converted in .tif and scale bars added using ImageJ software (NIH). At least 30 roots of each genotype were analyzed.

RESULTS

DRB7.2 is involved in endogenous IR-siRNA production

In order to gain insights into the function of DRB7.2, we performed genome-wide small RNA profiling on wild-type Col-0 and *drb7.2* mutant flowers, by small RNA sequencing of two independent biological replicates. We first examined the distribution of sRNAs that perfectly match the *Arabidopsis* genome, excluding rRNA and tRNA, and found no major differences in the global size distribution of total reads between *drb7.2* and Col-0 plants (Figure 1A and Supplementary Table S2), apart from a slight decrease in the amount of 22 nt-long sRNAs that might be correlated with the slight increase in the amount of 24 nt-long siRNA.

Next, we sorted sRNAs into their major functional categories and normalized their abundance to the amount of the evolutionarily conserved DCL1-dependent miRNAs (68), whose accumulation is not affected by the *drb7.2* mutation (Figure 2A; (51)). We found that lack of DRB7.2 does not significantly impact the accumulation of ta-siRNAs or p4-siRNAs (Figure 1B). However, and in sharp contrast, the accumulation of endogenous IR-siRNAs was strongly altered in *drb7.2* mutant plants. This was characterized by (i) a global increase in the total amount of endoIR-siRNAs produced and (ii) a clear change in their accumulation pattern with, chiefly, a strong increase in the accumulation of DCL3-dependent 24 nt endoIR-siRNAs, compare to wild-type plants (Figure 1B and Supplementary Table S2). This specific effect of the *drb7.2* mutation was also evident when size distribution of sRNAs corresponding to three endogenous IR representative loci were analyzed (Figure 1C and Supplementary Table S2). This effect was also accompanied by a robust increase in DCL4-dependent 21 nt endoIR-siRNAs (Figure 1B), although not on all endogenous IR loci (Supplementary Table S2). Collectively, these observations suggest that DRB7.2 is, somehow, specifically involved in endoIR-siRNA production.

Northern analysis of various representatives of the different classes of endogenous sRNAs confirmed the results of sRNA sequencing. Indeed, in the *drb7.2* mutant background, the steady-state levels of DCL1-dependent miRNAs, DCL4-dependent ta-siRNAs and miRNAs, and DCL3-dependent p4-siRNAs were similar to the WT control Col-0 (Figure 2A). By contrast, the accumulation pattern of endogenous IR-siRNAs was clearly altered in *drb7.2* mutant plants, with a strong increase in DCL3-dependent 24 nt IR-siRNA levels and a more modest, but visible, increase in DCL4-dependent 21 nt IR-siRNA (Figure 2A and Supplementary Figure S1). Interestingly, a similar pattern of endoIR-siRNA accumulation was also observed in the *drb4* mutant background (Figure 2A and Supplementary Figure S1), indicating that both DRB4 and DRB7.2 regulate the processing of endogenous IR transcripts.

Increased 24 nt IR-siRNA accumulation is not caused by a change in the homeostasis of DCL3

The above results prompted us to investigate whether the global increase in endoIR-derived siRNA accumulation observed in *drb7.2* (Figure 1B) and *drb4* (47), and the change in their accumulation pattern (Figures 1B, C and 2A), could result from a modification in the steady-state level of one, or more, of the sRNA-producing DCLs. To test this hypothesis, we assessed protein levels of DCL3 and DCL4, which are responsible for the production of the 24 nt and 21 nt siRNAs from endogenous IR loci, respectively. Unfortunately, despite several attempts, we were not able to obtain specific antibodies directed against DCL2 and, therefore, its accumulation could not be tested. We also decided to assess the accumulation of DCL1 because DCL1 has been previously shown to optimize the processing of IRs, presumably by facilitating access and subsequent processing by the other DCLs (50). Western blot analysis revealed that DCL1, DCL3 and DCL4 steady-state levels were similar in *drb7.2* and *drb4* to those found in control plants (Figure 2B), indicating that the altered accumulation of endoIR-derived siRNA observed in *drb7.2* or *drb4* does not result from a change in the homeostasis of those processing factors.

Similar observations were made for AGO1 and AGO4 accumulation, the two main Argonaute proteins that load and potentially stabilize, 21/22 nt and 24 nt endoIR-siRNAs, respectively (Figure 2B). Finally, based on its interaction with DRB7.2 (51) and their similar pattern of IR-siRNA accumulation, we also assessed the level of DRB4 and found that its accumulation was slightly decreased in *drb7.2* mutant plants (Figure 2B). This effect does not result from decreased level of the DRB4 mRNA as assessed by qRT-PCR analyses (Figure 2C), and is most likely due to destabilization and/or increased turn-over of the pool of DRB4 normally in complex with DRB7.2 (see below). Of note, this lower amount of DRB4 observed in *drb7.2* does not impact the production of DCL4/DRB4-dependent sRNAs such as *TAS1* or *TAS3* ta-siRNAs and miR822 (Figure 2A), indicating that DRB4 is not a limiting factor for optimal DCL4 activity on those precursors.

DRB4 forms specific and mutually exclusive complexes with DRB7.2 or DCL4

Based on the concerted evolution of DCL4 and DRB7.2 dsRBM, we previously tested a potential interaction between these two proteins by bimolecular fluorescence complementation. In these experiments, we observed that DRB7.2 interacts strongly with DRB4 but not with DCL4, whereas DRB4 was found to interact with both DRB7.2 and DCL4 (51). These observations, together with the change in endoIR-siRNA production, but not of other DCL4/DRB4-dependent sRNAs, found in *drb7.2* mutant plants (Figure 2A), suggested that DRB4 might be partitioned into two distinct cellular pools, one specifically interacting with DCL4 and the other with DRB7.2, where it fulfils other/specific function(s). However, an equally plausible explanation was that DCL4 specifically requires DRB7.2 as a cofactor, in addition to DRB4, for efficient processing of IR transcripts. Loss of either DRBs would then alter DCL4 activity on IR precursors and concurrently stimulate DCL3-mediated production of the 24 nt endoIR-siRNAs. This latter possibility entails that DRB7.2 interacts indirectly with DCL4, most likely through its association with DRB4, a possibility that was not previously addressed. Indeed, the bimolecular fluorescence complementation strategy is not the best suited approach to detect in-

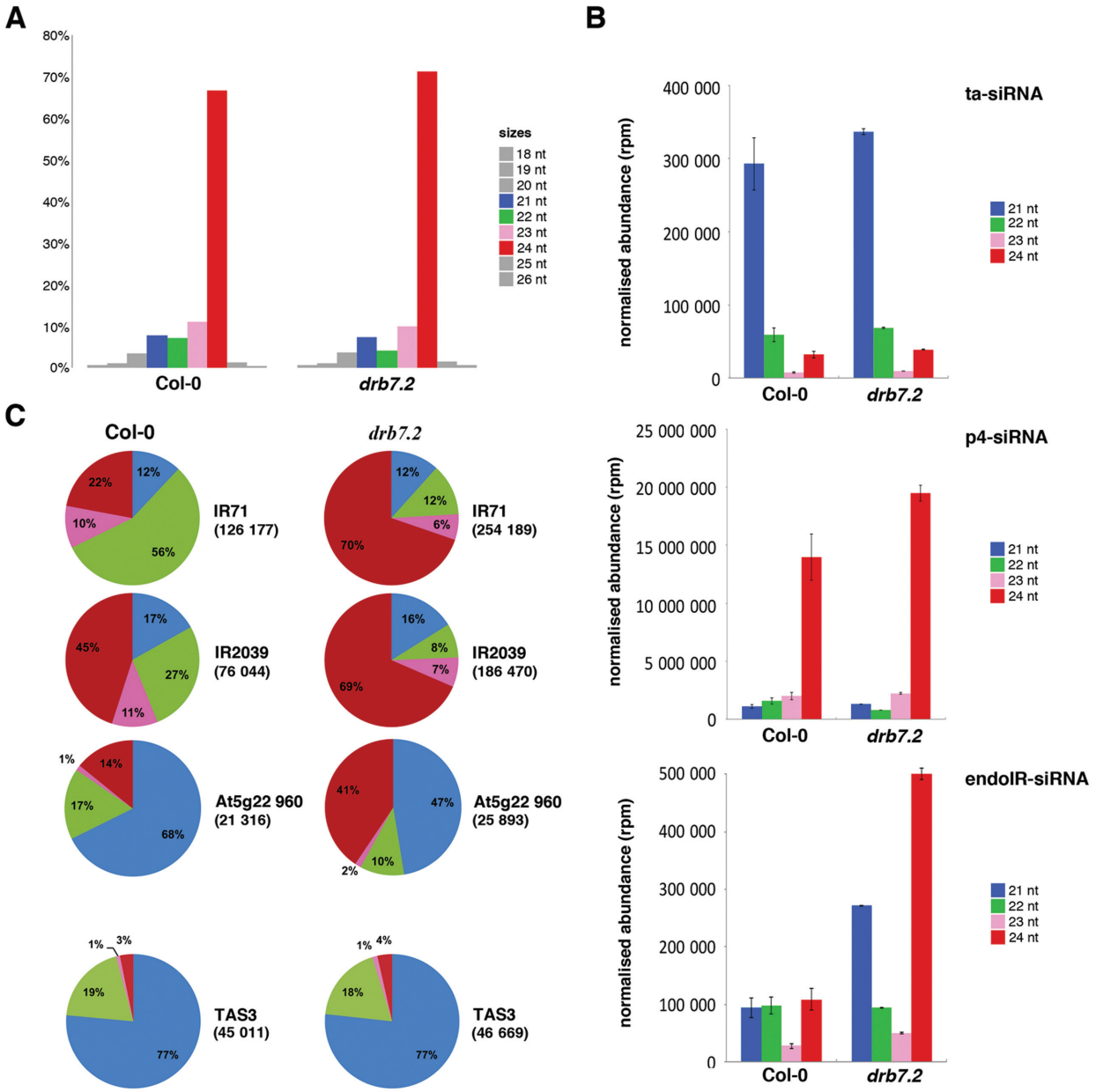

Figure 1. *drb7.2* mutant plants display altered accumulation of endoIR-siRNA. Wild-type (Col-0) and *drb7.2* mutant plants were subjected to high throughput sequencing. (**A**) Size distribution of small RNA reads that perfectly match the Arabidopsis nuclear genome, excluding rRNA and tRNA. The proportion of each size of small RNA is indicated by a color code: 21 nt (blue), 22 nt (green), 23 nt (pink), 24 nt (red) and grey for 18 to 20 nt and 25 to 26 nt. (**B**) Normalized small RNA abundance of the three major classes of endogenous siRNAs. Small RNAs from Col-0 and *drb7.2* mutant plants were classified as ta-siRNAs (upper panel), p4-siRNAs (middle panel) or endoIR-siRNAs (lower panel) based on published annotation and their abundance was normalized to the total amount of conserved miRNAs. The color code of small RNA size is the same as in (A). (**C**) Normalized size distribution of endoIR-siRNAs from three IR loci (IR71, IR2039 and AT5G22960). Size distribution of TAS3-derived ta-siRNAs is shown here as a control. Numbers of normalized small RNA reads that perfectly match the aforementioned loci are represented under bracket. The color code of small RNA size is the same as in (A). Graphs in (B) were obtained using the mean value of the two biological replicates and error bars indicate the variation observed between the two replicates.

direct protein–protein interactions as it requires very close proximity of the N- and C-terminal YFP moieties fused to the proteins tested, in order to reconstitute a functional YFP and fluorescent signal.

Therefore, in order to discriminate between these two possibilities we decided to perform co-immunoprecipitation (co-IP) experiments. For that purpose, we first generated transgenic *Arabidopsis* lines expressing functional, epitope-tagged versions of DRB7.2 or DCL4. Transgenes expressing, under the control of the 35S promoter or its own promoter, the genomic sequence of DRB7.2 fused in C-terminal to GFP (35S:*DRB7.2:GFP*/*drb7.2* or *pDRB7.2:DRB7.2:GFP*/*drb7.2*) rescued the *drb7.2* mutation and restored IR-siRNA production back to WT levels (Figures 3A and 6E). Similarly, a transgene expressing, under its own promoter, the genomic sequence of

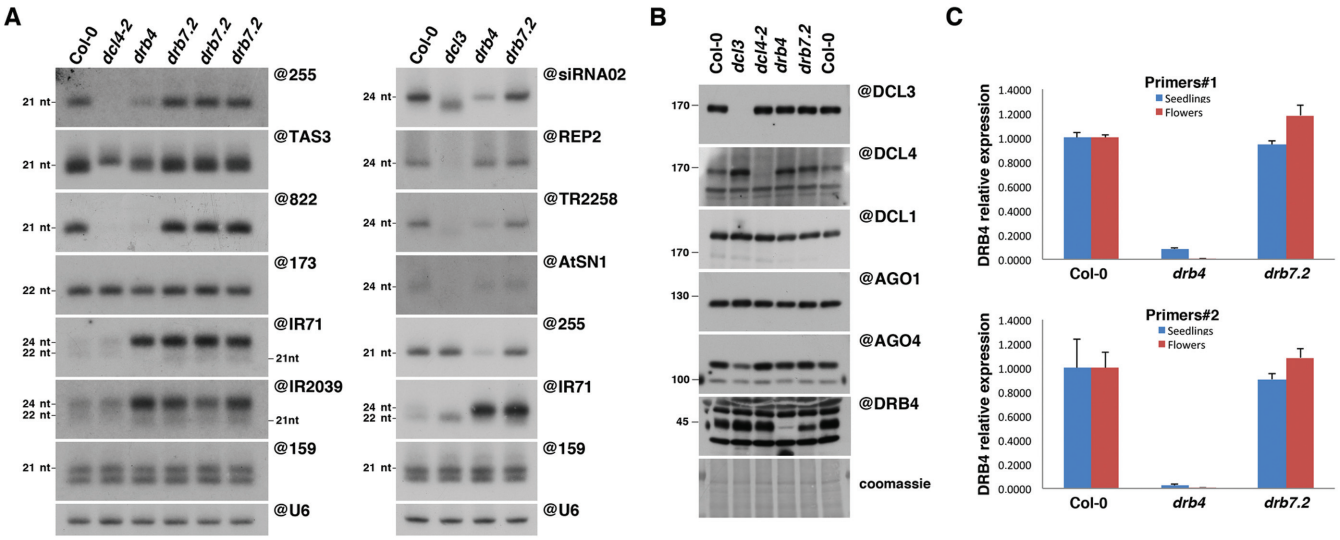

Figure 2. Effect of the *drb7.2* mutation on endogenous small RNAs or RNA silencing factor accumulation. (**A**) Northern blot analysis of trans-acting siRNA (@255, @TAS3), DCL4-dependent miRNA (@822), DCL1-dependent miRNA (@173, @159), endoIR-derived siRNA (@IR71, @IR2039) and DCL3-dependent p4-siRNA (@siRNA02, @REP2, @TR2558, @AtSN1) accumulation in wild-type (Col-0), *dcl4-2*, *drb4*, *drb7.2* or *dcl3* mutant plants was performed by sequential rounds of probing and stripping the same membranes. Please note that the three lanes labelled as *drb7.2* on the left blots correspond to three independent biological replicates. Accumulation of small RNA U6 (@U6) is used as loading control. (**B**) Accumulation of endogenous DCL3, DCL4, DCL1, AGO1, AGO4 and DRB4 was assessed by protein blot analysis of wild type, *dcl4-2*, *dcl3*, *drb4* and *drb7.2* plants. Equal loading was verified by Coomassie staining of the membrane after Western blotting. (**C**) Quantitative real-time PCR of the DRB4 mRNA accumulation in wild type, *drb4* and *drb7.2* plants. The mRNA level was normalized to that of *Actin2* (At3g18780) and then to the WT plants that was arbitrarily set to 1. Error bars represent standard deviation from two independent experiments in which triplicate PCRs were performed. Figure source data can be found with the Supplementary Data.

DCL4 fused in C-terminal to two Flag and two HA tags (pDCL4:*DCL4:FHA*/*dcl4*) complemented the phenotypic and molecular defects of the *dcl4* mutation (Figure 3A). Importantly, in these plants, DRB4 was efficiently immunoprecipitated with both DRB7.2:GFP and DCL4:FHA (Figure 3B and C). Collectively, these results indicate that both fusion proteins retain their biological functions and could, therefore, be used for co-IP experiments.

We, thus, generated transgenic plants expressing both DRB7.2:GFP and DCL4:FHA (*DRB7.2:GFP+DCL4:FHA*/*dcl4*). For that purpose, we introduced into our pDCL4:*DCL4:FHA*/*dcl4* transgenic line the DRB7.2:GFP transgene by agrotransformation and selected transformants that accumulate similar amount of DRB7.2:GFP than the one found in our transgenic line only expressing the DRB7.2:GFP transgene. Despite efficient immunoprecipitation of either recombinant protein, no DRB7.2:GFP signal could be detected in the IP fraction of DCL4:FHA (Figure 3B) and, conversely, no DCL4:FHA signal could be detected in the IP fraction of DRB7.2:GFP (Figure 3C), indicating that DRB7.2 and DCL4 are not able to interact *in planta*, even in the presence of DRB4. These results support the existence of specific and mutually exclusive DRB4-containing complexes that differ by their association with either DRB7.2 or DCL4. Further support to this hypothesis was provided when we compared the amount of DRB4 immunoprecipitated by DRB7.2:GFP, in the presence or absence of DCL4:FHA. Despite similar levels of immunoprecipitated DRB7.2:GFP, a strong reduction of the DRB4 signal was observed in the co-IP fraction of plants co-expressing DCL4:FHA (Figure 3C), suggesting that DCL4 and DRB7.2 compete for interaction with DRB4 and that DRB4 has a higher affinity for DCL4 than for DRB7.2. In line with this assumption, similar levels of DRB4 were detected in IP fractions of DCL4:FHA, in presence or absence of DRB7.2:GFP (Figure 3B), further indicating that DCL4 outcompetes DRB7.2 for the interaction with DRB4. Finally, IP fractions of DRB7.2:GFP were also sent to mass spectrometry analysis in order to identify the protein partners of DRB7.2. DRB4 was found to be the top scoring protein with very high coverage (Supplementary Table S2) and spectral count whereas no peptide corresponding to DCL4 (or of any of the other DCLs) was retrieved (Montavon and Dunoyer, unpublished observations). Collectively, these findings indicate that DRB7.2 interacts with DRB4 in a complex that does not contain DCL4 and strongly suggest the existence of, at least, two distinct cellular pools of DRB4.

The DRB4/DRB7.2 complex represses IR processing by the siRNA-generating DCLs

The strong and specific increase of DCL3-dependent 24 nt endoIR-siRNAs levels observed in both *drb4* and *drb7.2* mutants (Figure 2A) suggests that the DRB4/DRB7.2 complex may act as a specific repressor of DCL3 processing on IR substrates.

To address this genetically, we compared the accumulation of endoIR-siRNAs in mutants carrying genetic lesions in each of the three siRNA-generating DCL genes (*DCL2-4*), or combinations thereof, with the one found in *drb7.2* single mutant, or *drb7.2*/*dcl2*, *drb7.2*/*dcl3* and *drb7.2*/*dcl4*

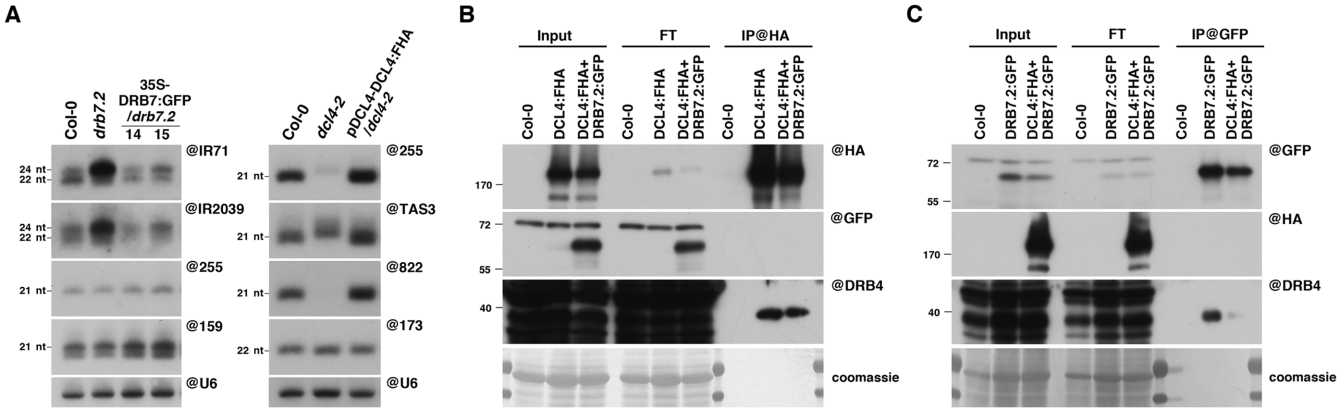

Figure 3. DRB4 interacts in a mutually exclusive manner with DCL4 and DRB7.2. (**A**) Northern analysis of endoIR-siRNA (@IR71, @IR2039), trans-acting siRNA (@255, @TAS3), DCL4-dependent miRNA (@822) and DCL1-dependent miRNA (@173, @159) accumulation in wild-type, *dcl4-2*, *drb7.2*, DRB7.2:GFP or DCL4:FHA-expressing plants was performed by sequential rounds of probing and stripping the same membranes. Accumulation of small RNA U6 (@U6) is used as loading control. (**B**) Immunoprecipitation experiments were conducted in wild-type, DCL4:FHA or DRB7.2:GFP+DCL4FHA-expressing plant using a HA-specific antibody. Co-IP of DRB7.2:GFP and DRB4 was examined by Western blot analyses using appropriate antibodies. Coomassie staining of the same membrane was used as a loading control. (**C**) Immunoprecipitation experiments were conducted in wild-type, DRB7.2:GFP or DRB7.2:GFP+DCL4FHA-expressing plant using a GFP-specific antibody. Co-IP of DCL4:FHA and DRB4 was examined by Western blot analyses using appropriate antibodies. Coomassie staining of the same membrane was used as a loading control. Figure source data can be found with the Supplementary Data.

double mutants (Figure 4A). A similar comparison was also performed using *drb4* single or *drb4/dcl2*, *drb4/dcl3* and *drb4/dcl4* double mutants (Figure 4B). Northern analysis of endogenous IR-siRNAs in these various mutant backgrounds revealed that the amount of 24 nt IR-siRNA produced in *dcl2* (Figure 4A and B) or *dcl2/4* mutants (Figure 4C), where DCL3 is, respectively, the prevalent or the only remaining DCL that processes endogenous IR, were similar to the one found in WT control plants. By contrast, loss-of-function mutation in DRB4 or DRB7.2, either alone or in combination with the *dcl2* or *dcl4* mutations, triggers a huge increase in DCL3-dependent 24 nt IR-siRNA production (Figure 4A and B). Moreover, no additive effect on the accumulation of those sRNAs was observed in the *drb4/drb7.2* double mutant (Figure 4D), supporting the hypothesis that DRB4 and DRB7.2 act together, as part of the same complex, to repress DCL3 processing.

Most likely, this effect does not entail direct interaction of the DRB4/DRB7.2 complex with DCL3 given that DRB4 does not interact *in vivo* with DCL3 (47), and that no peptides corresponding to DCL3 were retrieved in the mass spectrometry analysis of DRB7.2 immunoprecipitates (Montavon and Dunoyer, unpublished observations). Yet, when either component of the DRB4/DRB7.2 complex is absent, DCL3 becomes, somehow, much more efficient in processing those long dsRNA precursors and outcompetes DCL2/DCL4 for endogenous IR-siRNA production (Figures 2A and 4).

Of note, this inhibitory effect only occurs on endoIR-siRNA production, as DCL3-dependent p4-siRNA were unaffected in *drb7.2* or *drb7.2/dcl2* mutant backgrounds (Figures 2A and 4A). This comparison cannot be made for all p4-siRNAs with plants containing the *drb4* and/or *dcl4* mutation as it was shown previously (47), and confirmed in this study (Figure 4), that these mutants exhibit, for currently unknown reason, reduced accumulation of some of those sRNAs. However, similar conclusions can be reached for REP2-derived p4-siRNAs that are not affected by the *dcl4* or *drb4* mutations, confirming the specificity of the inhibitory effect mediated by the DRB4/DRB7.2 complex.

Interestingly, we also noticed a strong increase of the 22 nt endoIR-siRNA accumulation in *drb7.2/dcl3* and *drb4/dcl3* double mutants compared to the one found in *dcl3* or *dcl34* mutants where DCL2 is, respectively, the prevalent or the only remaining DCL that processes endogenous IR (Figure 4A–C). These results indicate that the DRB4/DRB7.2 complex is also acting as a repressor of DCL2 processing on IR substrates, when DCL3 is absent.

In order to assess the effect of DRB7.2 on exogenous siRNA accumulation, wild-type Col-0 and *drb7.2* mutant plants were also infected with either *Turnip crinkle virus* or *Tobacco rattle virus*. Northern analysis revealed that neither vsiRNAs production nor viral RNA accumulation were affected by the *drb7.2* mutation (Supplementary Figure S2), indicating that DRB7.2 is not involved in the plant antiviral RNA silencing response.

The DRB4/DRB7.2 complex represses IR-siRNA production by specifically sequestering their long dsRNA precursors

Next, we sought to determine how the DRB4/DRB7.2 complex represses DCL3 and DCL2 processing on IR substrates. A direct interaction of this complex with DCL3 and DCL2 is rather unlikely based on the mass spectrometry analyses of DRB7.2 immunoprecipitated fraction, and on the documented lack of interaction between DRB4 and DCL3 (47). Therefore, based on their intrinsic property to bind dsRNA, we rather reasoned that the DRB4/DRB7.2 complex might directly sequester specific dsRNA precursors, thereby preventing their access and processing by DCL3 and/or DCL2.

To test this hypothesis, we performed RNA immunoprecipitation (RIP) experiments using *drb7.2* transgenic lines

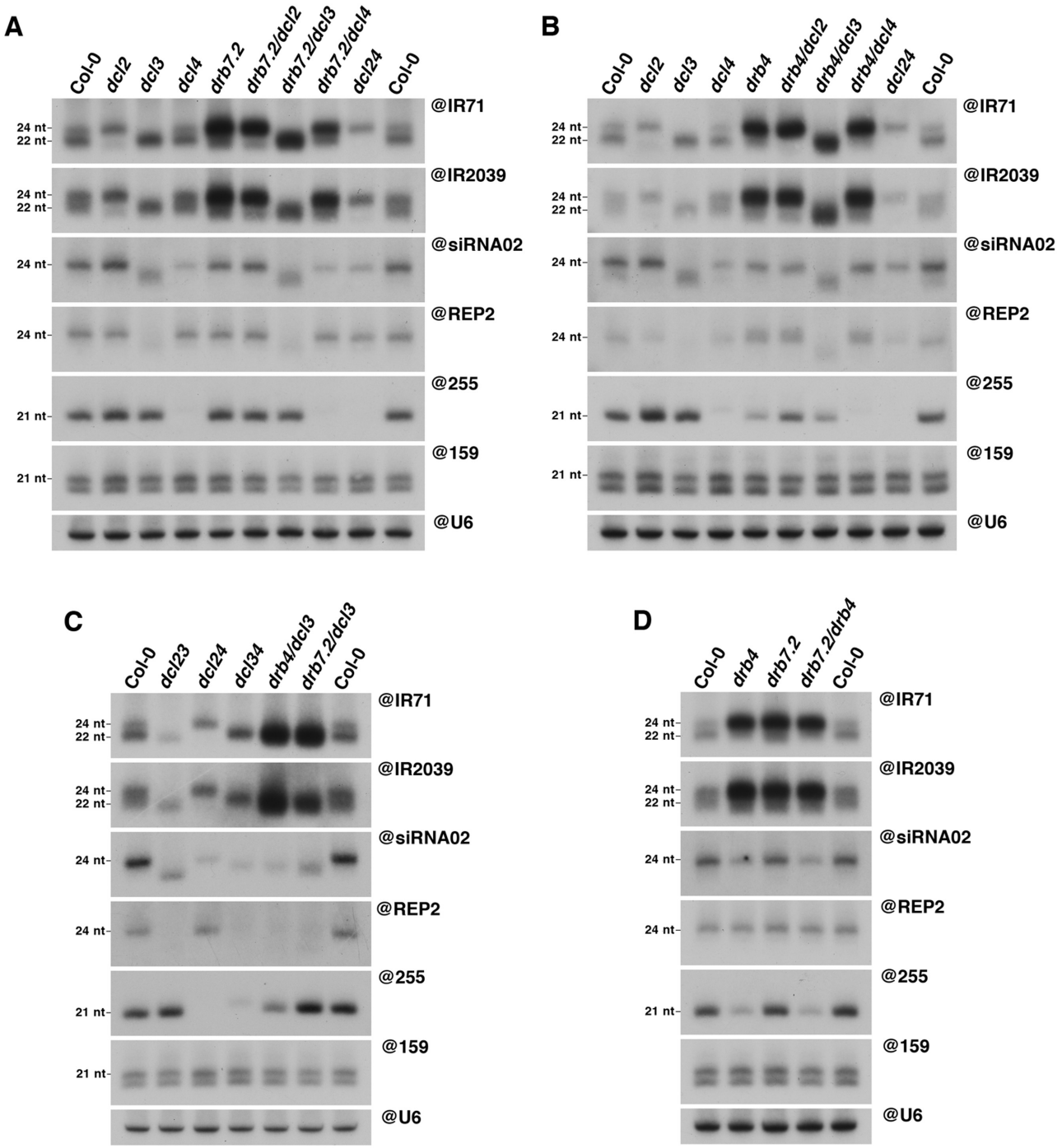

Figure 4. The DRB4/DRB7.2 complex specifically represses DCL3 and DCL2-dependent production of endoIR-siRNAs. (**A**) RNA gel blot analysis of endoIR-siRNA (@IR71, @IR2039), p4-siRNA (@REP2, @siRNA02) and trans-acting siRNA (@255) accumulation in wild-type, *dcl2*, *dcl3*, *dcl4*, *drb7.2*, *drb7.2/dcl2*, *drb7.2/dcl3*, *drb7.2/dcl4* and *dcl2/4* mutant plants was performed by sequential rounds of probing and stripping the same membranes. (**B**) Accumulation of the same small RNAs depicted in (A) was assessed in wild-type, *dcl2*, *dcl3*, *dcl4*, *drb4*, *drb4/dcl2*, *drb4/dcl3*, *drb4/dcl4* and *dcl2/4* mutant plants. (**C**) Similar analysis to the one depicted in (A) was performed in wild-type, *dcl2/3*, *dcl2/4*, *dcl3/4*, *drb4/dcl3* and *drb7.2/dcl3* plants. (**D**) Similar analysis to the one depicted in (A) was performed in wild-type, *drb4*, *drb7.2* and *drb7.2/drb4* plants. Accumulation of the DCL1-dependent miR159 (@159) and small RNA U6 (@U6) were used as loading control. Figure source data can be found with the Supplementary Data.

expressing DRB7.2:GFP (Figure 3A). As a positive control for these RIP experiments, we decided to use a *dcl4* transgenic line expressing a mutated version of DCL4, DCL4-8, fused in C-terminal to GFP (pDCL4:*DCL4-8:GFP*/*dcl4*). This allele carries a G to A transition within the DEAD helicase domain of DCL4 (leading to G610D mutation; (50)) that impairs production of all the DCL4-dependent sRNAs, despite producing a stable protein (Supplementary Figure S3). Importantly, this mutant allele is still able to bind and stabilize the DCL4 dsRNA substrates such as *TAS1*, miR822 or endoIR-siRNA precursors (Figure 5). In parallel, 35S-*GFP* expressing plants were used as negative control.

Immunoprecipitation of DRB7.2:GFP followed by Northern blot analysis allowed us to detect a specific signal corresponding to IR71 and IR2039 RNA precursors in the IP fraction, indicating that DRB7.2 is indeed able to bind endoIR-siRNAs precursors (Figure 5). Importantly, and by contrast with DCL4-8, no signal corresponding to the precursors of *TAS1* ta-siRNA or miRNA822 were found associated with DRB7.2 (Figure 5), in agreement with the unaltered accumulation of their associated sRNAs in the *drb7.2* mutant. In parallel, we also noticed that the signal detected for endoIR precursors in the DCL4-8:GFP IP fraction was more heterogeneous in size than the one detected in the DRB7.2:GFP IP fraction (Figure 5). Given that (i) endo-IR precursors are processed by the three siRNA-generating DCLs, chiefly DCL2 and DCL3, and (ii) that this heterogeneity was not observed for the other precursors bound by DCL4-8, whose processing is purely DCL4-dependent (such as *TAS1* ta-siRNA and miRNA822 precursors, Figure 5), this most likely reflects binding by DCL4-8 to IR dsRNAs that have been already partially processed by the two other siRNA-generating DCLs. Finally, neither DCL1-dependent miRNA precursors nor DCL3-dependent p4-siRNA precursors could be detected in the IP fraction of DRB7.2, indicating that this protein specifically binds precursors of endoIR-siRNAs but not of other sRNAs (Figure 5 and Supplementary Figure S4). Therefore, the strict correlation between the altered accumulation of endoIR-siRNAs observed in the *drb7.2* mutant and the specificity of the precursors bound by DRB7.2, strongly support our hypothesis that DRB7.2 selectively sequesters endoIR precursors.

Moreover, band-shift experiments (Supplementary Figure S5A), as well as RIP experiments followed by RNase A/T1 treatment, that selectively cleave single-stranded RNAs (ssRNAs) but do not digest dsRNAs (Supplementary Figure S5B), revealed that DRB7.2 has a higher affinity for the latter *in vitro* and binds them *in vivo*. This supports that the endoIR-siRNA precursors bound by DRB7.2 are sequestered under their dsRNA form.

DCL4 and DRB7.2 compete for DRB4 binding

The above results also suggest that DRB4 is partitioned between DCL4, where it acts as a cofactor for efficient production of DCL4-dependent sRNAs, and DRB7.2, where it functions to specifically sequester endogenous IR precursors and inhibit DCL3 and DCL2 processing of these substrates. Therefore, we reasoned that expressing a higher

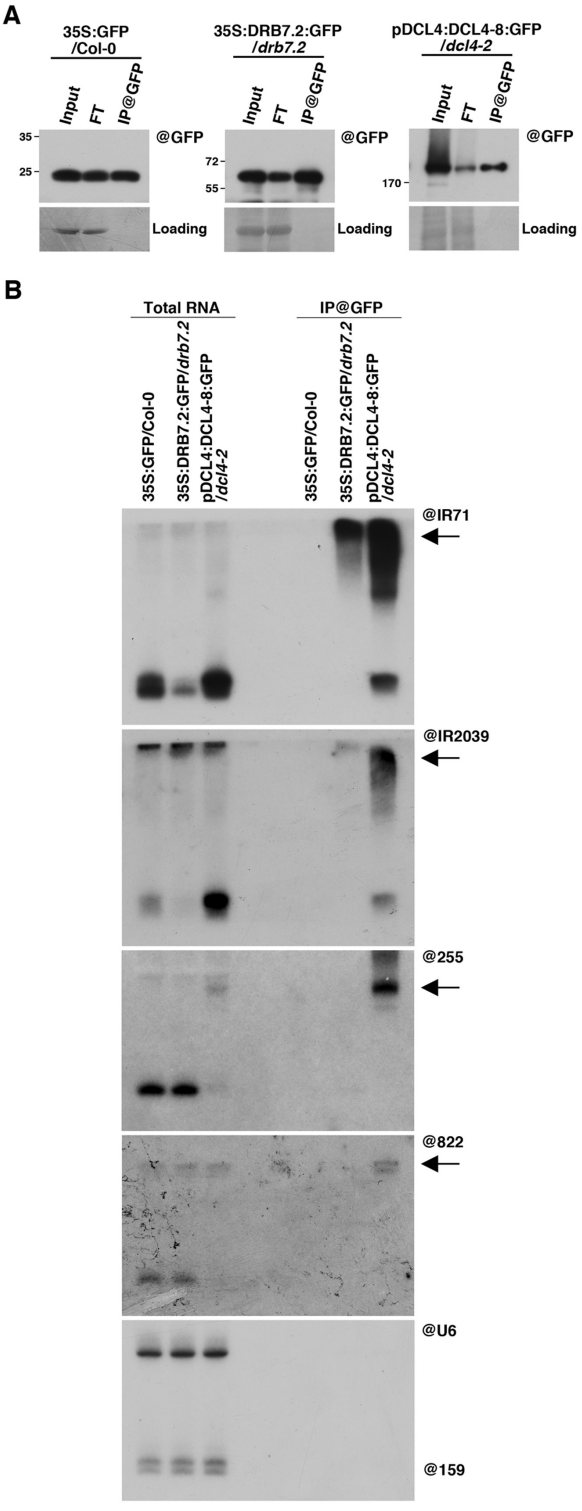

Figure 5. DRB7.2 specifically binds endoIR-siRNAs precursors. (**A**) Immunoprecipitation experiments were conducted in GFP-, DRB7.2:GFP- or DCL4-8:GFP-expressing plants using a GFP-specific antibody. The presence of the corresponding proteins in each IP was confirmed by protein blot analysis. (**B**) Total RNA extracted from the respective IPs was subjected to northern analysis using the indicated probes by sequential rounds of probing and stripping the same membrane. The signal corresponding to the sRNA precursors is indicated by an arrow. @U6: loading control. Figure source data can be found with the Supplementary Data.

amount than the endogenous level of one of the two DRB4 partners should result in displacing the equilibrium toward one or the other complex.

In agreement with this hypothesis, Northern analysis of endogenous IR-siRNA accumulation in *pDCL4:DCL4-8:GFP/dcl4* transgenic plants revealed a similar pattern to the one observed in the *drb7.2* mutant background, with a strong increase in the DCL3-dependent 24 nt siRNA species (Figures 5B and 6A). Using our DCL4 antibody, we confirmed by Western blot analysis that the amount of DCL4-8:GFP accumulating in this transgenic line was higher than the amount of endogenous DCL4 present in wild-type Col-0 plants (Figure 6B). To discard the possibility that this observation was, somehow, linked to the mutation carried by the DCL4-8 transgene, we repeated this analysis in transgenic plants expressing a wild-type functional version of DCL4 (*pDCL4:DCL4WT:GFP/dcl4*) that rescued the *dcl4* mutation and restored production of DCL4-dependent tasiRNAs and miRNAs back to WT levels (Figure 6A). Similar results were obtained in these transgenic plants, where higher levels of DCL4 than those found in wild-type Col-0 trigger an endoIR-siRNA accumulation pattern analogous to the one observed in *drb7.2* mutant (Figure 6A and B). This effect was further confirmed in a third, independent, transgenic line expressing, under the 35S promoter, a genomic copy of DCL4 (35S:DCL4) (Figure 6C and D). Collectively, these results suggest that, by expressing DCL4 at a higher level, the DRB4 equilibrium is displaced toward an interaction with this protein, to the detriment of the DRB4/DRB7.2 complex formation. This results in a defect of IR dsRNA precursors sequestration leading to an increase in DCL3-dependent endoIR-siRNA production, similar to the one observed in *drb4* or *drb7.2* mutant plants. In agreement with this hypothesis, this altered endoIR-siRNA accumulation was not observed in *dcl4-8* mutant plants, where DCL4 accumulates to similar level as in wild-type plants (Supplementary Figure S3).

Conversely, expressing increasing amount of DRB7.2 should favor the formation of the DRB4/DRB7.2 complex. This should, in turn, promote the sequestration of more IR dsRNA precursors and translate into less endoIR-siRNAs produced. In agreement with this hypothesis, Northern analysis revealed that the accumulation of both DCL3-dependent 24 nt and DCL2-dependent 22 nt endoIR-siRNAs was indeed reduced in *35S:DRB7.2:GFP/drb7.2* transgenic lines compared to the level detected in *pDRB7.2:DRB7.2:GFP/drb7.2* (where, comparatively, DRB7.2:GFP accumulates to much lower level) or Col-0 plants (Figure 6E and F). As expected, based on the apparent higher affinity of DCL4, over DRB7.2, for DRB4 interaction (Figure 3), and on the observation that optimal DCL4 activity can still be obtained, even when lower amounts of DRB4 are available (Figure 2), no obvious effect on the accumulation of the purely DCL4/DRB4-dependent sRNAs could be detected in these transgenic lines (Figure 6E).

Collectively, the above results further substantiate the existence of two distinct pools of DRB4 that differ by their interaction with either DCL4 or DRB7.2.

Partitioning of DRB4 between DCL4 and DRB7.2 occurs in distinct subcellular compartments

Given that DRB4 was previously shown to accumulate in both nucleus and cytoplasm (48), we next sought to address if the partitioning of DRB4 between DRB7.2 and DCL4 occurred in the same, or distinct, subcellular compartment(s). For this purpose, we analyzed by confocal microscopy the subcellular localization of DRB7.2 and DCL4, in transgenic plants expressing functional GFP fusion of either protein.

DRB7.2 localization was found to be purely nuclear in both *35S:DRB7.2:GFP/drb7.2* and *pDRB7.2:DRB7.2:GFP/drb7.2* transgenic lines. As shown in Figure 7A–D, DRB7.2 is uniformly distributed throughout the nucleoplasm and found enriched in discrete nuclear foci that may correspond to previously described 'siRNA-processing centers' or 'Dicing bodies' (72,73). Strikingly, and in sharp contrast to the DRB7.2 nuclear localization, DCL4 was found to be mostly cytoplasmic in *pDCL4:DCL4WT:GFP/dcl4* transgenic plants (Figure 7E and F). In addition, and as previously described when expressed under the control of its native endogenous promoter (74,75), DCL4 was, on occasions, also observed in the nucleus, almost exclusively in discrete nuclear foci. A similar localization pattern was also observed for DCL4-8, indicating that this mutation does not affect DCL4 localization (Figure 7G and H).

Collectively, these observations indicate that DCL4 and DRB7.2 are mostly located in distinct subcellular compartments and strongly suggest that DRB4 is partitioned between the nucleus and the cytoplasm to form specific complexes. Of note, the DCL4 localization observed here differs from the purely nuclear localization reported earlier, where DCL4 was expressed under the control of strong constitutive promoter (32,76), suggesting that genetic information regulating DCL4 localization might be embedded within its native promoter sequence and emphasizing the importance of using an endogenous promoter to accurately assess protein localization. In line with these assumptions, it has indeed recently been shown that DCL4 endogenous promoter exhibits a discrete methylation patch that influences the transcriptional start site of this gene (77). In a wild-type situation, this methylated promoter leads to the production of the cytoplasmic DCL4 observed here (Figure 7E and F), whereas removal of this methylation patch (e.g. in mutants of the RNA-directed DNA methylation pathway, or through the use of an alternative promoter) leads to the production of a DCL4 isoform extended by a 61 amino acids, containing a nuclear localization signal (77).

DISCUSSION

This study not only unravels the function of DRB7.2, a new player in plant RNA silencing pathways, it also provides additional information regarding DRB4, one of the best-characterized plant DRB, by uncovering a new cellular function of this protein.

DRB4 was previously seen as a mere cofactor of DCL4, mainly required to promote efficient production of various DCL4-dependent sRNAs, whereas DRB7.2, one of the two members of a newly identified DRB family conserved

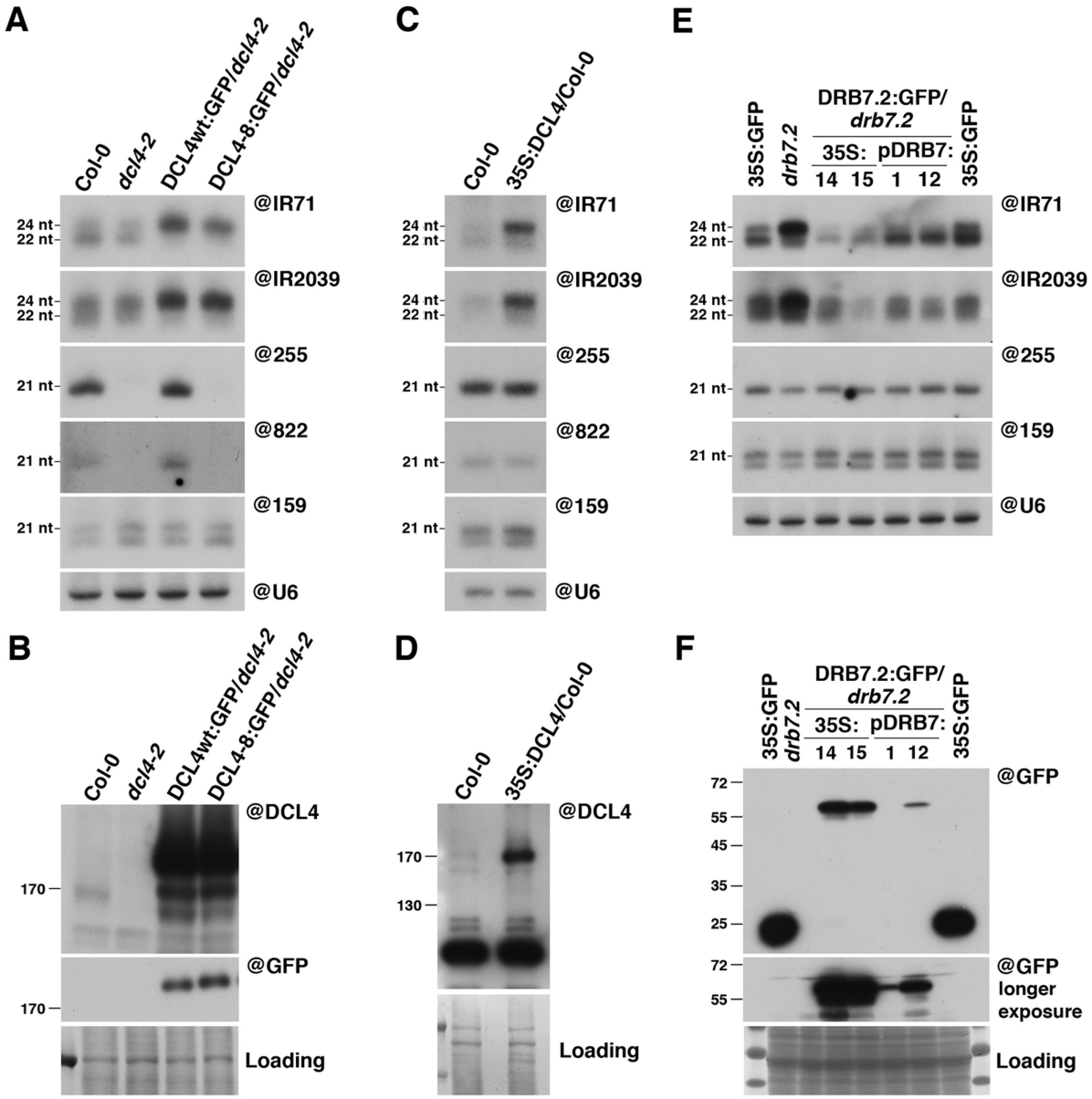

Figure 6. Effect of DCL4 or DRB7.2 overaccumulation on endogenous small RNA levels. (**A**) Northern analysis of endoIR-derived siRNA (@IR71, @IR2039), trans acting siRNA (@255) and DCL4-dependent miRNA (@822) accumulation in wild-type, *dcl4-2* and transgenic plants expressing DCL4wt:GFP or DCL4-8:GFP was performed by sequential rounds of probing and stripping the same membranes. (**B**) DCL4 accumulation was visualized by Western blotting using a DCL4- or GFP-specific antibody. (**C**) RNA gel analysis in wild-type or 35S:DCL4 transgenic plants using the same probes as in (A). (**D**) Over accumulation of the DCL4 protein was confirmed by protein blot analysis using a DCL4-specific antibody. (**E**) Accumulation of endo-IR siRNA and trans-acting siRNA was assessed by Northern blot in 35S:GFP-, 35S:DRB7.2:GFP- (two independent transgenic lines, #14 and #15) or pDRB7.2:DRB7.2:GFP- (two independent transgenic lines, #1 and #12) expressing plants by sequential rounds of probing and stripping the same membranes. (**F**) Accumulation of GFP or DRB7.2:GFP protein was verified by Western blot. For RNA blot, miR159 and U6 were used as loading control. For protein blot, Coomassie staining of membranes were used to verify equal loading. Figure source data can be found with the Supplementary Data.

in all vascular plants, had no clear role in RNA silencing. Here, we show that these two DRBs play together an important role in endoIR-siRNA production by negatively regulating the processing of their dsRNA precursors. All together, the findings that (i) DRB4 and DRB7.2 physically associate in a complex that does not contain DCL4 (Figure 3), (ii) that both *drb4* and/or *drb7.2* mutants display the same change in the accumulation pattern of endoIR-siRNA (Figure 4), and (iii) that DRB7.2 specifically binds the precursors of endoIR-siRNA but not of other sRNAs (Figure 5), indicate that this regulation is achieved through the formation of a DRB4/DRB7.2 complex that selectively binds to, and most likely sequesters, endoIR-siRNA precursors, thereby preventing their access and processing by the siRNA-generating DCLs, chiefly DCL3. Although not assessed in the present study, the increased accumulation of 24 nt easiRNA species previously observed in the *drb7.2/ddm1* double mutant (51) may also suggest that, at

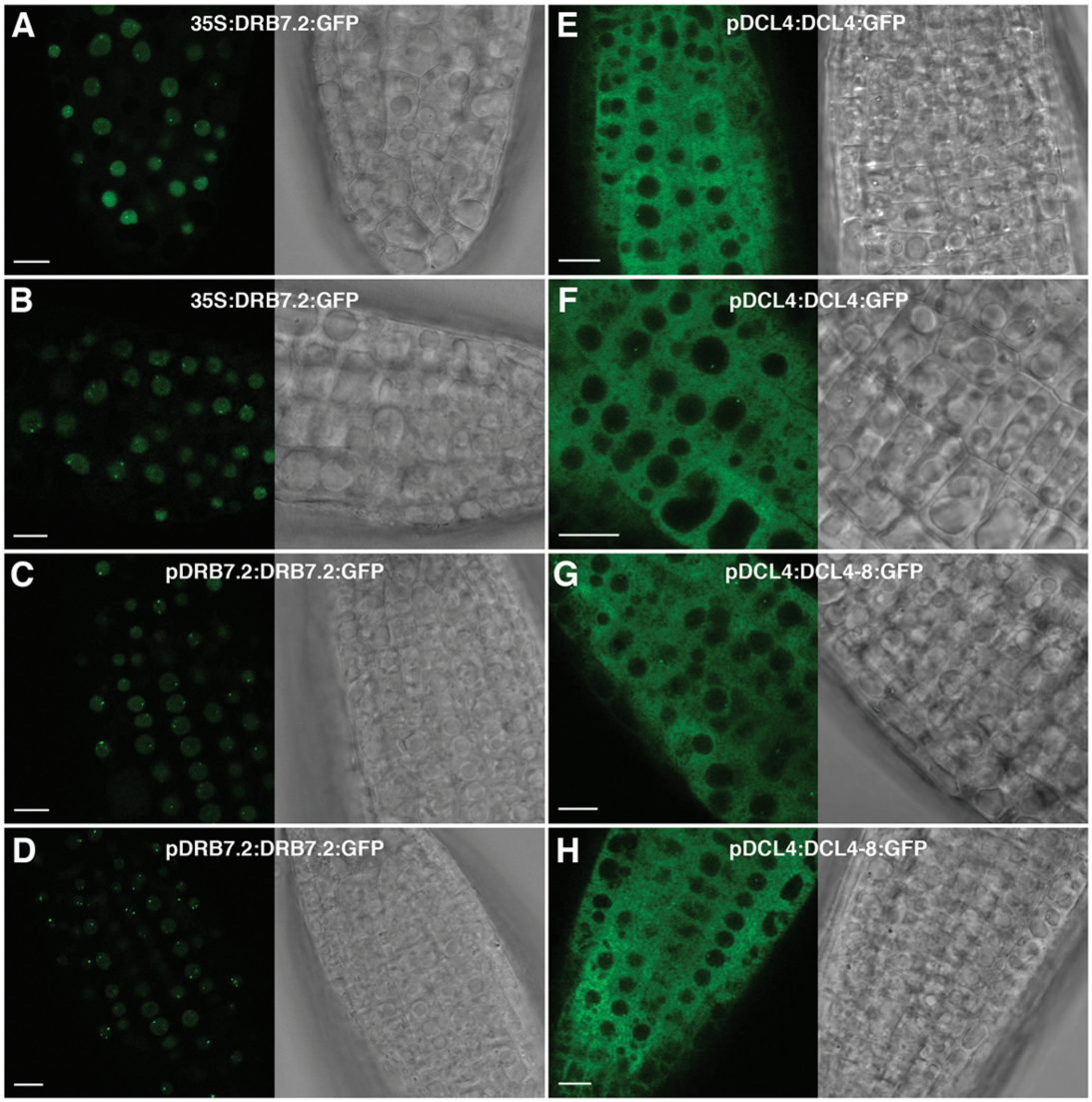

Figure 7. DRB7.2 and DCL4 localize in distinct subcellular compartments. Confocal microscope images of GFP in root tips of (**A** and **B**) 35S-DRB7.2:GFP-, (**C** and **D**) pDRB7.2-DRB7.2:GFP-, (**E** and **F**) pDCL4-DCL4:GFP- or (**G** and **H**) pDCL4-DCL4-8:GFP- transgenic lines. Scale bar = 50 μm.

least, some of the easiRNA precursors can be sequestered by the DRB4/DRB7.2 complex.

While the reason(s) for the selectivity of the DRB4/DRB7.2 complex is still unknown, differences in terms of dsRNA size, structure and/or subcellular localization can potentially explain its specific effect. For instance, although both are produced in the nucleus, endoIR-siRNA precursors are long perfect or near perfect, dsRNA molecules whereas p4-siRNAs are generated from short dsRNA precursors, 27–50 nt in length. Interestingly, band-shift assays, performed with purified DRB7.2, showed that this protein displays stronger affinity for long (>150 bp) dsRNA as compared to smaller species (<80 bp) (Supplementary Figure S6). This observation may, therefore, explain the lack of binding of p4-siRNA precursors by DRB7.2 (Supplementary Figure S4) and, consequently, the unaltered accumulation of p4-siRNAs in the *drb7.2* mutant (Figure 2). A similar rationale may also explain the lack of DRB7.2 binding to miRNA precursors, which have short imperfect stem-loop structures. Moreover, miRNA precursors contain several mismatches and bulges that may also affect the affinity of DRB7.2 for a given dsRNA. Alternatively, DRB1 affinity for miRNA precursors may outcompete DRB7.2 for their binding. Finally, precursors of ta-siRNAs are long perfect dsRNA, structurally similar in essence to those of endoIR-siRNA. However, *TAS* dsRNA precursors being, most likely, generated in cytoplasmic foci containing the different key factors required for their synthesis, such as SGS3 and RDR6 (76,78), this localization may preclude a potential binding by DRB7.2, which is exclusively nuclear (Figure 6).

In line with this latter observation, the findings that DRB7.2 and DCL4 (i) are localized in different subcellular compartments (Figure 7), (ii) associate with DRB4 in a mutually exclusive manner (Figure 3) and (iii), when overexpressed, compete for DRB4 binding (Figure 6), strongly

support the existence of, at least, two distinct cellular pools of DRB4. These two pools fulfil different and specific functions, e.g. promoting DCL4-dependent sRNA production in the cytoplasm and repressing endoIR-siRNA production in the nucleus, which agrees with the documented nucleocytoplasmic localization of DRB4 (48). In addition, the recent report that DRB4 seems to be required for the formation of the discrete nuclear foci of DCL4 (77) may either suggest the existence of a third cellular pool of DRB4 of currently unknown function, or that a small proportion of the DRB4 partitioning between DCL4 and DRB7.2 described here, may also occur in the nucleus.

These findings are reminiscent to the distinct cellular pools of AGO1 that were shown to specifically interact with either siRNA or miRNA and that were differentially affected by viral suppressors of RNA silencing (64). Although in the case of AGO1, the reason for this specificity is still unknown, these observations, together with the findings made in the present study, stress the importance of addressing the properties of a given RNA silencing factor with respect to its subcellular localization and/or complex composition in order to reveal specific and/or discrete cellular functions. In this respect, characterizing the function of the other DRB7.2-interacting partners, identified in our mass spectrometry analysis, may provide additional information or reveal new function for this protein. Moreover, this study, together with the recent role ascribed to non-DCL RNase three-like (RTL) proteins, RTL1 and RTL2, in modulation of sRNA production (79,80), shed light on new layers of regulation and the ever-growing complexity, of plant RNA silencing pathways. In connection with this, it will be interesting to assess the function and biological role of the other member of the DRB7 family (DRB7.1) that still awaits characterization. Based on its nuclear localization, it might be also important to assess if DRB7.2 affect somehow the accumulation of DNA viruses that replicate in this subcellular compartment.

Finally, our results also reveal that plants have evolved a specific DRB complex to modulate selectively the production of endoIR-siRNAs (Figures 1 and 2, Supplementary Table S2 and Supplementary Figure S7). In addition to illustrating how endogenous IR loci constitute useful molecular probes of the mechanisms of RNA silencing, the existence of such a complex put into question the function of those particular sRNA precursors, particularly in the light of the absence of any obvious developmental defects observed in *drb7.2* mutant plants. Indeed, so far, endogenous IRs with an extended fold-back structure have been mostly considered as relatively ill-defined, primary steps in the evolution of young MIRNA loci (68,81). They have also been regarded as having little, if any, regulatory potential of their own, notably because they were thought to be expressed at low or very low levels to avoid the off-targeting effects of their associated siRNA populations (2,81).

Although these assumptions might be true in some cases, small RNA deep-sequencing analysis revealed that at least some specific IR loci are in fact transcribed at high levels (Figure 1). The function of the DRB4/DRB7.2 complex could, therefore, be to dampen the production of endoIR-siRNAs from those particular loci in order to minimize potential off-targeting effects with deleterious consequences. In addition, the DRB4/DRB7.2 complex could help prevent highly expressed endoIRs from titrating away all the DCL2 and DCL3 available in the cell, leaving these DCLs free to perform their conventional roles in siRNA biogenesis. Alternatively, and perhaps more appealingly, some of the sRNAs produced from those endogenous IR loci may have regulatory functions that might help plants to respond and cope more efficiently to changes in their environment. Any external stimuli, such as biotic or abiotic stresses, leading to a change in the accumulation, or the availability, of either components of the DRB4/DRB7.2 complex will then translate into the rapid release of the sequestered precursors and quick production of their associated sRNAs, allowing the plants to potentially respond more efficiently to the perceived stress. In that case, the role of the DRB4/DRB7.2 complex could then be seen as a safety reservoir for precursors of sRNAs involved in adapting sequence-specific plant responses to stress, which might be particularly important at specific developmental stages or in discrete cell types. This hypothesis will undoubtedly deserve in-depth investigation in the future.

SUPPLEMENTARY DATA

Supplementary Data are available at NAR Online.

ACKNOWLEDGEMENTS

The authors thank N. Pumplin for sharing his pDCL4:DCL4:GFP constructs before publication; R. Wagner's team for plant care; Baptiste Monsion and the P3P platform for help in protein production and members of the IBMP for critical reading of the manuscript.

FUNDING

Agence Nationale pour la Recherche [ANR-14-CE19-0014-01 to P.D.]; LABEX NetRNA [ANR-10-LABX-0036_NETRNA] from the French National Research Agency as part of the Investments for the future program; French Ministry of Research [T.M.]. Funding for open access charge: ANR [ANR-14-CE19-0014-01].
Conflict of interest statement. None declared.

REFERENCES

1. Baulcombe,D.C. (2004) RNA silencing in plants. *Nature*, **431**, 356–363.
2. Voinnet,O. (2009) Origin, biogenesis, and activity of plant microRNAs. *Cell*, **136**, 669–687.
3. Chapman,E.J. and Carrington,J.C. (2007) Specialization and evolution of endogenous small RNA pathways. *Nat. Rev. Genet.*, **8**, 884–896.
4. Allen,E., Xie,Z., Gustafson,A.M. and Carrington,J.C. (2005) microRNA-Directed phasing during trans-acting siRNA biogenesis in plants. *Cell*, **121**, 207–221.
5. Yoshikawa,M., Peragine,A., Park,M.Y. and Poethig,R.S. (2005) A pathway for the biogenesis of trans-acting siRNAs in Arabidopsis. *Genes Dev.*, **19**, 2164–2175.
6. Gasciolli,V., Mallory,A.C., Bartel,D.P. and Vaucheret,H. (2005) Partially redundant functions of Arabidopsis DICER-like enzymes and a role for DCL4 in producing trans-acting siRNAs. *Curr. Biol.*, **15**, 1494–1500.

7. Blevins,T., Podicheti,R., Mishra,V., Marasco,M., Tang,H. and Pikaard,C.S. (2015) Identification of Pol IV and RDR2-dependent precursors of 24 nt siRNAs guiding de novo DNA methylation in Arabidopsis. *eLife*, **4**, e09591.
8. Zhai,J., Bischof,S., Wang,H., Feng,S., Lee,T.F., Teng,C., Chen,X., Park,S.Y., Liu,L., Gallego-Bartolome,J. *et al.* (2015) A one precursor one siRNA Model for Pol IV-dependent siRNA biogenesis. *Cell*, **163**, 445–455.
9. Kasschau,K.D., Fahlgren,N., Chapman,E.J., Sullivan,C.M., Cumbie,J.S., Givan,S.A. and Carrington,J.C. (2007) Genome-wide profiling and analysis of Arabidopsis siRNAs. *PLoS Biol.*, **5**, e57.
10. Lindow,M., Jacobsen,A., Nygaard,S., Mang,Y. and Krogh,A. (2007) Intragenomic matching reveals a huge potential for miRNA-mediated regulation in plants. *PLoS Comput. Biol.*, **3**, e238.
11. Bologna,N.G. and Voinnet,O. (2014) The diversity, biogenesis, and activities of endogenous silencing small RNAs in Arabidopsis. *Ann. Rev. Plant Biol.*, **65**, 473–503.
12. Baumberger,N. and Baulcombe,D.C. (2005) Arabidopsis ARGONAUTE1 is an RNA Slicer that selectively recruits microRNAs and short interfering RNAs. *Proc. Natl. Acad. Sci. U.S.A.*, **102**, 11928–11933.
13. Brodersen,P., Sakvarelidze-Achard,L., Bruun-Rasmussen,M., Dunoyer,P., Yamamoto,Y.Y., Sieburth,L.E. and Voinnet,O. (2008) Widespread translational inhibition by plant miRNAs and siRNAs. *Science*, **320**, 1185–1190.
14. Mallory,A. and Vaucheret,H. (2010) Form, function, and regulation of ARGONAUTE proteins. *Plant Cell*, **22**, 3879–3889.
15. Law,J.A. and Jacobsen,S.E. (2010) Establishing, maintaining and modifying DNA methylation patterns in plants and animals. *Nat. Rev. Genet.*, **11**, 204–220.
16. Szittya,G., Moxon,S., Pantaleo,V., Toth,G., Rusholme Pilcher,R.L., Moulton,V., Burgyan,J. and Dalmay,T. (2010) Structural and functional analysis of viral siRNAs. *PLoS Pathog.*, **6**, e1000838.
17. Qi,X., Bao,F.S. and Xie,Z. (2009) Small RNA deep sequencing reveals role for *Arabidopsisthaliana* RNA-Dependent RNA Polymerases in Viral siRNA Biogenesis. *PloS One*, **4**, e4971.
18. Donaire,L., Wang,Y., Gonzalez-Ibeas,D., Mayer,K.F., Aranda,M.A. and Llave,C. (2009) Deep-sequencing of plant viral small RNAs reveals effective and widespread targeting of viral genomes. *Virology*, **392**, 203–214.
19. Morel,J.B., Godon,C., Mourrain,P., Beclin,C., Boutet,S., Feuerbach,F., Proux,F. and Vaucheret,H. (2002) Fertile hypomorphic ARGONAUTE (ago1) mutants impaired in post-transcriptional gene silencing and virus resistance. *Plant Cell*, **14**, 629–639.
20. Qu,F., Ye,X. and Morris,T.J. (2008) Arabidopsis DRB4, AGO1, AGO7, and RDR6 participate in a DCL4-initiated antiviral RNA silencing pathway negatively regulated by DCL1. *Proc. Natl. Acad. Sci. U.S.A.*, **105**, 14732–14737.
21. Jaubert,M., Bhattacharjee,S., Mello,A.F., Perry,K.L. and Moffett,P. (2011) ARGONAUTE2 mediates RNA-silencing antiviral defenses against Potato virus X in Arabidopsis. *Plant Physiol.*, **156**, 1556–1564.
22. Wang,X.-B., Jovel,J., Udomporn,P., Wang,Y., Wu,Q., Li,W.-X., Gasciolli,V., Vaucheret,H. and Ding,S.-W. (2011) The 21-nucleotide, but not 22-nucleotide, viral secondary small interfering RNAs direct potent antiviral defense by two cooperative argonautes in *Arabidopsisthaliana*. *Plant Cell*, **23**, 1625–1638.
23. Harvey,J.J.W., Lewsey,M.G., Patel,K., Westwood,J.H., Heimstädt,S., Carr,J.P. and Baulcombe,D.C. (2011) An antiviral defense role of AGO2 in plants. *PloS One*, **6**, e14639.
24. Carbonell,A., Fahlgren,N., Garcia-Ruiz,H., Gilbert,K.B., Montgomery,T.A., Nguyen,T., Cuperus,J.T. and Carrington,J.C. (2012) Functional analysis of three Arabidopsis ARGONAUTES using slicer-defective mutants. *Plant Cell*, **24**, 3613–3629.
25. Liu,Q., Rand,T.A., Kalidas,S., Du,F., Kim,H.E., Smith,D.P. and Wang,X. (2003) R2D2, a bridge between the initiation and effector steps of the Drosophila RNAi pathway. *Science*, **301**, 1921–1925.
26. Jiang,F., Ye,X., Liu,X., Fincher,L., McKearin,D. and Liu,Q. (2005) Dicer-1 and R3D1-L catalyze microRNA maturation in Drosophila. *Genes Dev.*, **19**, 1674–1679.
27. Han,M.H., Goud,S., Song,L. and Fedoroff,N. (2004) The Arabidopsis double-stranded RNA-binding protein HYL1 plays a role in microRNA-mediated gene regulation. *Proc. Natl. Acad. Sci. U.S.A.*, **101**, 1093–1098.
28. Czech,B. and Hannon,G.J. (2011) Small RNA sorting: matchmaking for Argonautes. *Nat. Rev. Genet.*, **12**, 19–31.
29. Vazquez,F., Gasciolli,V., Crete,P. and Vaucheret,H. (2004) The nuclear dsRNA binding protein HYL1 is required for microRNA accumulation and plant development, but not posttranscriptional transgene silencing. *Curr. Biol.*, **14**, 346–351.
30. Eamens,A.L., Smith,N.A., Curtin,S.J., Wang,M.-B. and Waterhouse,P.M. (2009) The *Arabidopsisthaliana* double-stranded RNA binding protein DRB1 directs guide strand selection from microRNA duplexes. *RNA*, **15**, 2219–2235.
31. Manavella,P.A., Hagmann,J., Ott,F., Laubinger,S., Franz,M., Macek,B. and Weigel,D. (2012) Fast-Forward Genetics Identifies Plant CPL Phosphatases as Regulators of miRNA Processing Factor HYL1. *Cell*, **151**, 859–870.
32. Hiraguri,A., Itoh,R., Kondo,N., Nomura,Y., Aizawa,D., Murai,Y., Koiwa,H., Seki,M., Shinozaki,K. and Fukuhara,T. (2005) Specific interactions between Dicer-like proteins and HYL1/DRB-family dsRNA-binding proteins in Arabidopsis thaliana. *Plant Mol. Biol.*, **57**, 173–188.
33. Kurihara,Y., Takashi,Y. and Watanabe,Y. (2006) The interaction between DCL1 and HYL1 is important for efficient and precise processing of pri-miRNA in plant microRNA biogenesis. *RNA*, **12**, 206–212.
34. Yang,S.W., Chen,H.-Y., Yang,J., Machida,S., Chua,N.-H. and Yuan,Y.A. (2010) Structure of Arabidopsis HYPONASTIC LEAVES1 and Its Molecular Implications for miRNA Processing. *Structure*, **18**, 594–605.
35. Qin,H., Chen,F., Huan,X., Machida,S., Song,J. and Yuan,Y.A. (2010) Structure of the Arabidopsis thaliana DCL4 DUF283 domain reveals a noncanonical double-stranded RNA-binding fold for protein-protein interaction. *RNA*, **16**, 474–481.
36. Song,L., Han,M.-H., Lesicka,J. and Fedoroff,N. (2007) *Arabidopsis* primary microRNA processing proteins HYL1 and DCL1 define a nuclear body distinct from the Cajal body. *Proc. Natl. Acad. Sci. U.S.A.*, **104**, 5437–5442.
37. Yang,X., Ren,W., Zhao,Q., Zhang,P., Wu,F. and He,Y. (2014) Homodimerization of HYL1 ensures the correct selection of cleavage sites in primary miRNA. *Nucleic Acids Res.*, **42**, 12224–12236.
38. Eamens,A.L., Kim,K.W., Curtin,S.J. and Waterhouse,P.M. (2012) DRB2 is required for microRNA biogenesis in Arabidopsis thaliana. *PloS One*, **7**, e35933.
39. Reis,R.S., Hart-Smith,G., Eamens,A.L., Wilkins,M.R. and Waterhouse,P.M. (2015) Gene regulation by translational inhibition is determined by Dicer partnering proteins. *Nat. Plants*, **1**, 14027.
40. Eamens,A.L., Wook Kim,K. and Waterhouse,P.M. (2012) DRB2, DRB3 and DRB5 function in a non-canonical microRNA pathway in Arabidopsis thaliana. *Plant Sign. Behav.*, **7**, 1224–1229.
41. Curtin,S.J., Watson,J.M., Smith,N.A., Eamens,A.L., Blanchard,C.L. and Waterhouse,P.M. (2008) The roles of plant dsRNA-binding proteins in RNAi-like pathways. *FEBS Lett.*, **582**, 2753–2760.
42. Raja,P., Jackel,J.N., Li,S., Heard,I.M. and Bisaro,D.M. (2014) Arabidopsis double-stranded RNA binding protein DRB3 participates in methylation-mediated defense against geminiviruses. *J. Virol.*, **88**, 2611–2622.
43. Fukudome,A., Kanaya,A., Egami,M., Nakazawa,Y., Hiraguri,A., Moriyama,H. and Fukuhara,T. (2011) Specific requirement of DRB4, a dsRNA-binding protein, for the in vitro dsRNA-cleaving activity of Arabidopsis Dicer-like 4. *RNA*, **17**, 750–760.
44. Nakazawa,Y., Hiraguri,A., Moriyama,H. and Fukuhara,T. (2007) The dsRNA-binding protein DRB4 interacts with the Dicer-like protein DCL4 in vivo and functions in the trans-acting siRNA pathway. *Plant Mol. Biol.*, **63**, 777–785.
45. Adenot,X., Elmayan,T., Lauressergues,D., Boutet,S., Bouché,N., Gasciolli,V. and Vaucheret,H. (2006) DRB4-dependent TAS3 trans-acting siRNAs control leaf morphology through AGO7. *Curr. Biol.*, **16**, 927–932.
46. Rajagopalan,R., Vaucheret,H., Trejo,J. and Bartel,D.P. (2006) A diverse and evolutionarily fluid set of microRNAs in Arabidopsis thaliana. *Genes Dev.*, **20**, 3407–3425.
47. Pelissier,T., Clavel,M., Chaparro,C., Pouch-Pelissier,M.N., Vaucheret,H. and Deragon,J.M. (2011) Double-stranded RNA binding proteins DRB2 and DRB4 have an antagonistic impact on polymerase IV-dependent siRNA levels in Arabidopsis. *RNA*, **17**, 1502–1510.

48. Jakubiec,A., Yang,S.W. and Chua,N.H. (2012) Arabidopsis DRB4 protein in antiviral defense against Turnip yellow mosaic virus infection. *Plant J.*, **69**, 14–25.
49. Zhu,S., Jeong,R.D., Lim,G.H., Yu,K., Wang,C., Chandra-Shekara,A.C., Navarre,D., Klessig,D.F., Kachroo,A. and Kachroo,P. (2013) Double-stranded RNA-binding protein 4 is required for resistance signaling against viral and bacterial pathogens. *Cell Rep.*, **4**, 1168–1184.
50. Dunoyer,P., Himber,C., Ruiz-Ferrer,V., Alioua,A. and Voinnet,O. (2007) Intra- and intercellular RNA interference in Arabidopsis thaliana requires components of the microRNA and heterochromatic silencing pathways. *Nat. Genet.*, **39**, 848–856.
51. Clavel,M., Pelissier,T., Montavon,T., Tschopp,M.A., Pouch-Pelissier,M.N., Descombin,J., Jean,V., Dunoyer,P., Bousquet-Antonelli,C. and Deragon,J.M. (2016) Evolutionary history of double-stranded RNA binding proteins in plants: identification of new cofactors involved in easiRNA biogenesis. *Plant Mol. Biol.*, **91**, 131–147.
52. Slotkin,R.K., Vaughn,M.W., Borges,F., Tanurdžić,M., Becker,J.D., Feijó,J.A. and Martienssen,R.A. (2009) Epigenetic reprogramming and small RNA silencing of transposable elements in pollen. *Cell*, **136**, 461–472.
53. McCue,A.D., Nuthikattu,S. and Slotkin,R.K. (2013) Genome-wide identification of genes regulated in trans by transposable element small interfering RNAs. *RNA Biol.*, **10**, 1379–1395.
54. McCue,A.D., Panda,K., Nuthikattu,S., Choudury,S.G., Thomas,E.N. and Slotkin,R.K. (2015) ARGONAUTE 6 bridges transposable element mRNA-derived siRNAs to the establishment of DNA methylation. *EMBO J.*, **34**, 20–35.
55. Nuthikattu,S., McCue,A.D., Panda,K., Fultz,D., DeFraia,C., Thomas,E.N. and Slotkin,R.K. (2013) The initiation of epigenetic silencing of active transposable elements is triggered by RDR6 and 21-22 nucleotide small interfering RNAs. *Plant Physiol.*, **162**, 116–131.
56. Creasey,K.M., Zhai,J., Borges,F., Van Ex,F., Regulski,M., Meyers,B.C. and Martienssen,R.A. (2014) miRNAs trigger widespread epigenetically activated siRNAs from transposons in Arabidopsis. *Nature*, **508**, 411–415.
57. Xie,Z., Johansen,L.K., Gustafson,A.M., Kasschau,K.D., Lellis,A.D., Zilberman,D., Jacobsen,S.E. and Carrington,J.C. (2004) Genetic and functional diversification of small RNA pathways in plants. *PLoS Biol.*, **2**, e104.
58. Xie,Z., Allen,E., Wilken,A. and Carrington,J.C. (2005) DICER-LIKE 4 functions in trans-acting small interfering RNA biogenesis and vegetative phase change in Arabidopsis thaliana. *Proc. Natl. Acad. Sci. U.S.A.*, **102**, 12984–12989.
59. Deleris,A., Gallego-Bartolome,J., Bao,J., Kasschau,K.D., Carrington,J.C. and Voinnet,O. (2006) Hierarchical action and inhibition of plant Dicer-like proteins in antiviral defense. *Science*, **313**, 68–71.
60. Himber,C., Dunoyer,P., Moissiard,G., Ritzenthaler,C. and Voinnet,O. (2003) Transitivity-dependent and -independent cell-to-cell movement of RNA silencing. *EMBO J.*, **22**, 4523–4533.
61. Clough,S.J. and Bent,A.F. (1998) Floral dip: a simplified method for Agrobacterium-mediated transformation of Arabidopsis thaliana. *Plant J.*, **16**, 735–743.
62. Yu,D., Fan,B., MacFarlane,S.A. and Chen,Z. (2003) Analysis of the involvement of an inducible Arabidopsis RNA-dependent RNA polymerase in antiviral defense. *Mol. Plant Microbe Interact.*, **16**, 206–216.
63. Thomas,C.L., Leh,V., Lederer,C. and Maule,A.J. (2003) Turnip crinkle virus coat protein mediates suppression of RNA silencing in Nicotiana benthamiana. *Virology*, **306**, 33–41.
64. Schott,G., Mari-Ordonez,A., Himber,C., Alioua,A., Voinnet,O. and Dunoyer,P. (2012) Differential effects of viral silencing suppressors on siRNA and miRNA loading support the existence of two distinct cellular pools of ARGONAUTE1. *EMBO J.*, **31**, 2553–2565.
65. Hurkman,W.J. and Tanaka,C.K. (1986) Solubilization of plant membrane proteins for analysis by two-dimensional gel electrophoresis. *Plant Physiol.*, **81**, 802–806.
66. Langmead,B., Trapnell,C., Pop,M. and Salzberg,S.L. (2009) Ultrafast and memory-efficient alignment of short DNA sequences to the human genome. *Genome Biol.*, **10**, R25.
67. Quinlan,A.R. and Hall,I.M. (2010) BEDTools: a flexible suite of utilities for comparing genomic features. *Bioinformatics*, **26**, 841–842.
68. Fahlgren,N., Howell,M.D., Kasschau,K.D., Chapman,E.J., Sullivan,C.M., Cumbie,J.S., Givan,S.A., Law,T.F., Grant,S.R., Dangl,J.L. *et al.* (2007) High-throughput sequencing of Arabidopsis microRNAs: evidence for frequent birth and death of MIRNA genes. *PloS One*, **2**, e219.
69. Griffiths-Jones,S., Grocock,R.J., van Dongen,S., Bateman,A. and Enright,A.J. (2006) miRBase: microRNA sequences, targets and gene nomenclature. *Nucleic Acids Res.*, **34**, D140–D144.
70. Mosher,R.A., Schwach,F., Studholme,D.J. and Baulcombe,D.C. (2008) PolIVb influences RNA-directed DNA methylation independently of its role in siRNA biogenesis. *Proc. Natl. Acad. Sci. U.S.A.*, **105**, 3145–3150.
71. Zhang,C., Li,G., Zhu,S., Zhang,S. and Fang,J. (2014) tasiRNAdb: a database of ta-siRNA regulatory pathways. *Bioinformatics*, **30**, 1045–1046.
72. Pontes,O., Li,C.F., Costa Nunes,P., Haag,J., Ream,T., Vitins,A., Jacobsen,S.E. and Pikaard,C.S. (2006) The Arabidopsis chromatin-modifying nuclear siRNA pathway involves a nucleolar RNA processing center. *Cell*, **126**, 79–92.
73. Fang,Y. and Spector,D.L. (2007) Identification of nuclear dicing bodies containing proteins for microRNA biogenesis in living Arabidopsis plants. *Curr. Biol.*, **17**, 818–823.
74. Pontes,O., Vitins,A., Ream,T.S., Hong,E., Pikaard,C.S. and Costa-Nunes,P. (2013) Intersection of small RNA pathways in Arabidopsis thaliana sub-nuclear domains. *PloS One*, **8**, e65652.
75. Hoffer,P., Ivashuta,S., Pontes,O., Vitins,A., Pikaard,C.S., Mroczka,A., Wagner,N. and Voelker,T. (2011) Posttranscriptional gene silencing in nuclei. *Proc. Natl. Acad. Sci. U.S.A.*, **108**, 409–414.
76. Kumakura,N., Takeda,A., Fujioka,Y., Motose,H., Takano,R. and Watanabe,Y. (2009) SGS3 and RDR6 interact and colocalize in cytoplasmic SGS3/RDR6-bodies. *FEBS Lett.*, **583**, 1261–1266.
77. Pumplin,N., Sarazin,A., Jullien,P., Bologna,N.G., Oberlin,S. and Voinnet,O. (2016) DNA methylation influences the expression of DICER-LIKE4 isoforms, which encode proteins of alternative localization and function. *Plant Cell*, doi:10.1105/tpc.16.00554.
78. Jouannet,V., Moreno,A.B., Elmayan,T., Vaucheret,H., Crespi,M.D. and Maizel,A. (2012) Cytoplasmic Arabidopsis AGO7 accumulates in membrane-associated siRNA bodies and is required for ta-siRNA biogenesis. *EMBO J.*, **31**, 1704–1713.
79. Shamandi,N., Zytnicki,M., Charbonnel,C., Elvira-Matelot,E., Bochnakian,A., Comella,P., Mallory,A.C., Lepere,G., Saez-Vasquez,J. and Vaucheret,H. (2015) Plants encode a general siRNA suppressor that is induced and suppressed by viruses. *PLoS Biol.*, **13**, e1002326.
80. Elvira-Matelot,E., Hachet,M., Shamandi,N., Comella,P., Saez-Vasquez,J., Zytnicki,M. and Vaucheret,H. (2016) Arabidopsis RNASE THREE LIKE2 modulates the expression of protein-coding genes via 24-nucleotide small interfering RNA-directed DNA methylation. *Plant Cell*, **28**, 406–425.
81. Allen,E., Xie,Z., Gustafson,A.M., Sung,G.H., Spatafora,J.W. and Carrington,J.C. (2004) Evolution of microRNA genes by inverted duplication of target gene sequences in Arabidopsis thaliana. *Nat. Genet.*, **36**, 1282–1290.